Leukemia regression by vascular disruption and antiangiogenic therapy

Gerard J. Madlambayan,[1,2] Amy M. Meacham,[1,2] Koji Hosaka,[2] Saad Mir,[1] Marda Jorgensen,[2] Edward W. Scott,[2] Dietmar W. Siemann,[3] and Christopher R. Cogle[1,2]

[1]Department of Medicine, Division of Hematology/Oncology, [2]Program in Stem Cell Biology and Regenerative Medicine, and [3]Department of Radiation Oncology, University of Florida, Gainesville

Acute myelogenous leukemias (AMLs) and endothelial cells depend on each other for survival and proliferation. Monotherapy antivascular strategies such as targeting vascular endothelial growth factor (VEGF) has limited efficacy in treating AML. Thus, in search of a multitarget antivascular treatment strategy for AML, we tested a novel vascular disrupting agent, OXi4503, alone and in combination with the anti-VEGF antibody, bevacizumab. Using xenotransplant animal models, OXi4503 treatment of human AML chloromas led to vascular disruption in leukemia cores that displayed increased leukemia cell apoptosis. However, viable rims of leukemia cells remained and were richly vascular with increased VEGF-A expression. To target this peripheral reactive angiogenesis, bevacizumab was combined with OXi4503 and abrogated viable vascular rims, thereby leading to enhanced leukemia regression. In a systemic model of primary human AML, OXi4503 regressed leukemia engraftment alone and in combination with bevacizumab. Differences in blood vessel density alone could not account for the observed regression, suggesting that OXi4503 also exhibited direct cytotoxic effects on leukemia cells. In vitro analyses confirmed this targeted effect, which was mediated by the production of reactive oxygen species and resulted in apoptosis. Together, these data show that OXi4503 alone is capable of regressing AML by a multitargeted mechanism and that the addition of bevacizumab mitigates reactive angiogenesis. (*Blood*. 2010; 116(9):1539-1547)

Introduction

Acute myelogenous leukemias (AMLs) often relapse despite initial disease remissions induced by conventional cytotoxic chemotherapies. Moreover, certain high-risk AMLs, such as those with activating mutations in *fms*-like tyrosine kinase receptor-3 (*FLT3*) and mixed lineage leukemia gene fusions are notoriously chemotherapy insensitive and prone to relapse.[1-3] Unfortunately, therapies targeting these mutant molecular pathways have only brought about modest clinical benefits.[4] Whereas many investigations have focused on the leukemia cell alone, a broader perspective taking into account the leukemia cell microenvironment may be needed to better appreciate leukemia pathobiology and conceive novel therapeutic strategies.

Clinically, the degree of angiogenesis in leukemia has prognostic utility. Increased levels of circulating angiogenic factors and increased microvessel density within leukemic bone marrow are high-risk indicators of disease relapse and early mortality.[5-9] It has also been reported that endothelial cells secrete soluble protein mediators such as granulocyte colony stimulating factor, granulocyte-macrophage colony stimulating factor, vascular endothelial growth factor (VEGF), and interleukin-6 (IL-6), which promote leukemia survival and proliferation.[10] Cell-cell interactions between endothelial cell adhesion molecules, like E-selectin, P-selectin, and VCAM-1, and leukemia cells may also propagate leukemia.[11,12] Reciprocally, leukemias induce angiogenesis and depend on neovessels for nutritive support.[13-17] Taken together, these data intimate the importance of functional blood vessel networks in leukemia progression.

To exploit the interrelationship between blood vessels and leukemia in a therapeutic approach, attempts have been made to interfere with the VEGF pathway in AML by inhibiting VEGF receptor tyrosine kinase activity and by binding VEGF isoforms.[18-22] In 2 feasibility studies, bevacizumab (Avastin; Genentech) was administered to patients with refractory AML and resulted in modest clinical benefit.[19,20]

Another approach to destabilizing leukemic blood vessels is to selectively target proliferating endothelial cells. Vascular disrupting agents (VDAs) represent a new class of agents, which target nascent blood vessels by directly binding microtubules in endothelial cells. Combretastatin (CA4P) was the first-in-class molecule that showed significant antineoplastic effects by destroying cancer-associated neovessels.[23,24] CA4P binds to β-tubulin subunits in proliferating endothelial cells and not resting endothelial cells, thereby selectively targeting neovascularization within cancer.[25-28] In solid tumor models, affected endothelial cells detach from the vascular wall leading to vascular collapse and tumor cell death due to blood flow obstruction. CA4P has also been administered in a preclinical model of leukemia and resulted in disease regression using a variety of leukemic cell lines via vascular disruption as well as direct cytotoxic effects mediated by the generation of reactive oxygen species (ROS).[29]

Recently, another combretastatin, OXi4503, has been identified that displays more potent vascular disruption and antitumor activity.[30,31] The enhanced antitumor activity of OXi4503 compared with CA4P has been ascribed to its efficacy not only in

Submitted June 29, 2009; accepted May 5, 2010. Prepublished online as *Blood* First Edition paper, May 14, 2010; DOI 10.1182/blood-2009-06-230474.

The publication costs of this article were defrayed in part by page charge payment. Therefore, and solely to indicate this fact, this article is hereby marked "advertisement" in accordance with 18 USC section 1734.

An Inside *Blood* analysis of this article appears at the front of this issue.

Table 1. Characteristics of AML specimens

Patient	Age, y	AML FAB subtype	Disease stage	Prior therapy	Antecedent hematologic disorder	Cell source	% blasts	Disease karyotype	Disease genetic analyses	Induction therapy	Disease response to induction
1	71	M1/2	Diagnosis	None	None	L-PB	> 98%	46, XY	FLT3-ITD$^+$,NPM-1$^+$	FLAG	Refractory
2	59	M1/2	Diagnosis	Decitabine	CMML	BM	70%	46, XY, del7(q32)	N/A	7+3	Refractory
3	74	M4	Diagnosis	Adriamycin, cyclophosphamide, taxotere, and XRT to chest wall for stage III breast cancer	None	BM	40%	46, XX t(6;11) (q27;q23)	FLT3-ITD$^-$, NPM-1$^-$, MLL$^+$	CECA	Refractory
4	66	M5	Relapse	7+3, HiDAC, allogeneic PBSCT	None	BM	60%	46, XY,del12(p11.2), t(15;21)(q22;q22)	FLT3-ITD$^+$, NPM-1$^-$	CECA	Remission
5	66	M2	Relapse	7+3	None	BM	50%	46, XX	FLT3-ITD$^+$, NPM-1$^+$	CECA	Refractory

AML indicates acute myelogenous leukemia; FAB, French American British; FLT3-ITD, Flt3 internal tandem duplication; NPM-1, nucleophosmin 1 mutation; MLL, mixed lineage leukemia mutation; CMML, chronic myelomonocytic leukemia; L-PB, leukopheresis of peripheral blood; BM, bone marrow; N/A, not applicable; FLAG, fludarabine, cytarabine, G-CSF; 7+3, cytarabine, idarubicin; CECA, cyclophosphamide, etoposide, carboplatin, cytarabine; HiDAC, high-dose cytarabine; and PBSCT, peripheral blood stem cell transplantation.

vascular disruption via microtubule binding but the potential for inducing cancer cell death resulting from the formation of reactive ortho-quinones that bind to cellular nucleophiles and form free radicals.[30-35] Despite the induction of significant tumor necrosis, all VDAs, including OXi4503, leave a thin layer of viable tumor tissue surviving at the tumor periphery.[35] These peripheral tumor cells, which survive due to nutritional support from surrounding normal vessels, are unaffected by VDA therapy and induce vigorous reactive angiogenesis supporting tumor regrowth.[35] Consequently, we have shown that in solid tumor models the combination of VDA therapy with antiangiogenic agents results in greater antitumor efficacy than is achievable with either treatment alone.[36]

Given the importance of neovascularization in leukemia and potent dual mechanisms of the novel OXi4503 molecule, we hypothesized that OXi4503 treatment may lead to regression in leukemia. To test this, we used in vivo models of human AML including a solid tumor chloroma model and a systemic model of primary human AML. The data show that OXi4503 was necessary to produce phenotypic and molecular remissions in systemic AML of differing subtypes including those with activating mutations in FLT3. Interestingly, the effects of OXi4503 on leukemia regression were through multiple mechanisms including vascular disruption and direct induction of leukemia cell apoptosis. In the chloroma model, additional treatment with bevacizumab was needed to induce similar disease response demonstrating that differences in the mechanisms of vascular disruption, reactive angiogenesis and cancer survival are active within these different leukemia models.

Methods

Patient specimens

Bone marrow (BM) and peripheral blood (PB) were donated by patients with AML of differing subtypes (Table 1) and cryopreserved according to approved protocols by the University of Florida Institutional Review Board. BM and PB from AML patients were removed from liquid nitrogen and quickly thawed in a 37°C water bath. Once thawed, cells were diluted 1:2 to 1:3 in Dulbecco phosphate-buffered saline (DPBS; Invitrogen) supplemented with 2% fetal bovine serum (FBS; Hyclone) and mononuclear cells (MNCs) were isolated by density centrifugation using Ficoll-Hypaque (Pharmacia). After separation, MNCs were washed in DPBS plus 2% FBS. Alternatively, MNCs were also isolated using a red cell lysis step. In this process, BM cells were thawed as described in DPBS plus 2% FBS. Cells were then centrifuged at 200*g* and resuspended 1:3 in red blood lysis buffer. After an additional centrifugation step, MNCs were resuspended in DPBS plus 2% FBS before use.

Xenotransplantation models

All animal studies were performed according to approved protocols from the University of Florida Institutional Animal Care and Use Committee. To test the efficacy of VDAs in human AML, human leukemia chimeras were established using NOD/scid/IL2R$\gamma^{-/-}$ (NOG) mice (The Jackson Laboratory). In the subcutaneous model, KG-1 cells were injected into dorsa of 8- to 10-week-old NOG mice. After 21 days of tumor growth, mice were randomly assigned to one of our treatment groups: control, bevacizumab alone, OXi4503 alone, and combination bevacizumab and OXi4503. Subcutaneous chloromas were measured by calipers for length and width every other day. Tumor volumes were calculated using the formula $(\pi \times W^2 \times L)/6$. After 2 weeks of treatment mice were euthanized and subcutaneous tumors harvested.

In the systemic model of leukemia, 8- to 10-week-old NOG mice were sublethally irradiated (325 cGy) and 10×10^6 to 50×10^6 AML MNCs of differing subtypes (Table 1) were intravenously injected within 4 to 24 hours of irradiation. After 6 weeks, mice were randomly assigned to 1 of

4 treatment groups: control, bevacizumab alone, OXi4503 alone, or combination OXi4503 plus bevacizumab. After 2 weeks of treatment, mice were euthanized and examined for human leukemia engraftment in their bone marrow using flow cytometry and polymerase chain reaction (PCR).

Therapeutic agents

OXi4503 (Oxigene) was dissolved in phosphate-buffered saline (PBS) and sodium bicarbonate, stored at 4°C and used within 48 hours of preparation. OXi4503 was administered at a dose of 10 mg/kg intraperitoneally 3 times a week for 2 weeks. Bevacizumab (Genentech) was stored at 4°C and administered at 4 mg/kg intraperitoneally weekly for 2 weeks.

Flow cytometry antibodies and analysis

To detect human hematopoietic engraftment in mouse BM, cells were stained with saturating amounts of anti–human CD45–fluorescein isothiocyanate and anti–human leukocyte antigens A, B, and C–allophycocyanin antibodies (BD Pharmingen) for 30 minutes on ice. Appropriate isotype controls were also used (BD Pharmingen). Stained cells were then washed, resuspended in DPBS plus 2% FBS containing Viaprobe and analyzed for surface markers and viable human cell content using a Becton Dickinson FACSCanto II flow cytometer. Transplanted NOG mice were scored positive if at least 0.1% of the BM cells collected expressed human CD45 and human leukocyte antigens A, B, and C. A total of 50 000 cells were analyzed per sample.

Cell viability assays

Leukemic KG-1 cells (ATCC) were seeded at 1×10^5 to 2×10^6 cells/mL in Iscove modified Dulbecco medium (IMDM) supplemented with 20% FBS. OXi4500 was added at the specified concentrations for 48 hours. In all in vitro studies, OXi4500 was used, which is the active, dephosphorylated form of OXi4503.[34] In addition to binding microtubules and causing depolymerization, OXi4500 can be oxidized to a reactive orthoquinone, which has the potential to form ROS and thereby result in cytotoxicity.[30-35] After incubation, viable cell numbers were determined using trypan blue dye exclusion.

To measure apoptosis, KG-1 cells were plated at 1×10^6 cells/mL in IMDM plus 20% FBS and incubated with OXi4500 at the concentrations indicated for 24 or 48 hours. Cells were then collected and stained using propidium iodide (PI) and annexin V–allophycocyanin (BD Pharmingen). Analysis was performed using a Becton Dickinson FACSCanto II flow cytometer.

Measurement of ROS generation

Intracellular ROS were detected after 48 hours of OXi4500 treatment. After treatment, KG1 cells were loaded with 2μM H2DCFDA (Molecular Probes) for 30 minutes at 37°C. After a 15-minute recovery in culture media, mean fluorescent intensity was measured by flow cytometry. Values were normalized to 0nM OXi4500 controls.

PCR

Genomic DNA was isolated from test samples using the Wizard Genomic DNA purification kit (Promega). Human *FLT3* internal tandem duplication (ITD) was amplified by single-step PCR using the New England BioLabs Taq PCR kit. The PCR mixture contained 100 ng of DNA, 500 pmol of each primer, 200μM DNTP solution mix, 1× Standard Taq Reaction Buffer with 1.5mM MgCl2, and 1 unit of *Taq* DNA Polymerase. For all reactions, denaturing, annealing, and extension steps were performed in a MJ Research PTC-100 thermocycler at 95°C for 30 seconds, 55°C for 30 seconds, and 72°C for 30 seconds, respectively, for 35 cycles including an initial 2-minute denaturing step at 95°C and a final extension step at 72°C for 5 minutes. Ten microliters of each PCR product were run on a 1% agarose gel and visualized under ultraviolet light after ethidium bromide staining. The *FLT3* wild-type produced a 328-bp band, whereas the *FLT3-ITD* produced a 400-bp band. Human glyceraldehyde 3-phosphate dehydrogenase (GAPDH) and mouse β-actin primers were used as housekeeping genes. Primer sequences are as follows: *hFLT* forward: GCAATTTAGGTATGAAAGCCAGC; *hFLT* reverse: CTTTCAGCATTTTGACGGCAACC *hGAPDH* forward: TCCAAAATCAAGTGGGGCGAT; *hGAPDH* reverse: TTCTAGACGGCAGGTCAGGTC mβ-actin forward: ATGGATGACGATATCGCT; mβ-actin reverse: ATGAGGTAGTCTGTCAGGT.

Immunohistochemistry of tumor sections

Harvested tissues were immersion-fixed overnight in 4% paraformaldehyde (PFA), after which bones were decalcified in 5% formic acid or 14% EDTA. All tissues were equilibrated overnight in 18% sucrose before being embedded in optimal cutting temperature (OCT) compound (Sakura Finetek USA). Prepared blocks were stored at −80°C and later cryosectioned at a thickness of 5 microns onto positively charged slides. Sections were air-dried overnight at room temperature before staining. A standard hemotoxylin and eosin stain (H&E) was done for each tissue.

Dual staining protocols were carried out sequentially under the following conditions. Where applicable, terminal deoxynucleotidyl transferase dUTP nick end labeling (TUNEL) staining was performed first using a commercially available assay kit (In Situ Cell Death Detection Kit Fluorescein; Roche Applied Sciences) following the manufacturer's instructions. Microwave irradiation in 0.01M citrate buffer pH 6.0 was used for the permeabilization step. A known positive tissue and 2 negative control slides were included in each run.

For immunostaining, optimal cutting temperature was removed from the slides with 1× Wash Solution (DakoCytomation) followed by antigen retrieval performed at 95°C for 20 minutes with a 20-minute cool down using Target Retrieval Solution (DakoCytomation). Slides were blocked in 3% horse serum for 30 minutes before the application of primary antibody overnight at 4°C. The antibodies used were rat anti–MECA-32 (1:10; BD Pharmingen), rabbit anti–human VEGF-A (Abcam), and rabbit anti–HIF 1α (1:150; Novus Biologicals). When dual staining with MECA and HIF 1α, it was possible to apply the 2 antibodies simultaneously and incubate as a cocktail. Staining with mouse anti–human CD45 (1:50; DakoCytomation) required the use of a mouse on mouse (M.O.M.) Standard Kit (Vector Laboratories). Slides initially stained by TUNEL were subjected to heat antigen retrieval at 95°C for 20 minutes before beginning the staining. Immunoreactivity was detected using 1:500 dilutions of species appropriate Alexa Fluor antibodies raised in donkey. In the case of HIF-1α and VEGF-A staining, anti–rabbit AlexaFluor 488 secondary was selected. For MECA-32, anti–rat Alexa Fluor 594 secondary was used. Staining with CD45 required the use of streptavidin Alexa Fluor 594, also at 1:500. Positive control tissues and concentration matched Ig controls were included with each immunoassay. Sections were mounted in VectaShield with DAPI before imaging.

Tissue analysis

Tissues were examined at room temperature using a fluorescent Leica DM 2500 microscope (Leica Microsystems) mounted with an Optronics color camera (Optronics) and analyzed with MagnaFire 2.1C software (Optronics). Objectives used were 10×/0.40, 20×/0.70, 40×/0.75, or 63×/1.20 (water-corrected objective). Slides were mounted with Vectashield containing 4′-6-diamidino-2-phenylindole (DAPI; Vector Laboratories). Quantification of microvessels was performed by counting number of MECA-32$^+$ blood vessels in 10 high-magnification (40×) fields of 5 specimens for each of 4 cohorts.

Statistics

Statistical differences between different experimental groups were determined by 1-way analysis of variance and the Student *t* test. The reported values represent the mean plus or minus SEM. A *P* value less than .05 was considered significant.

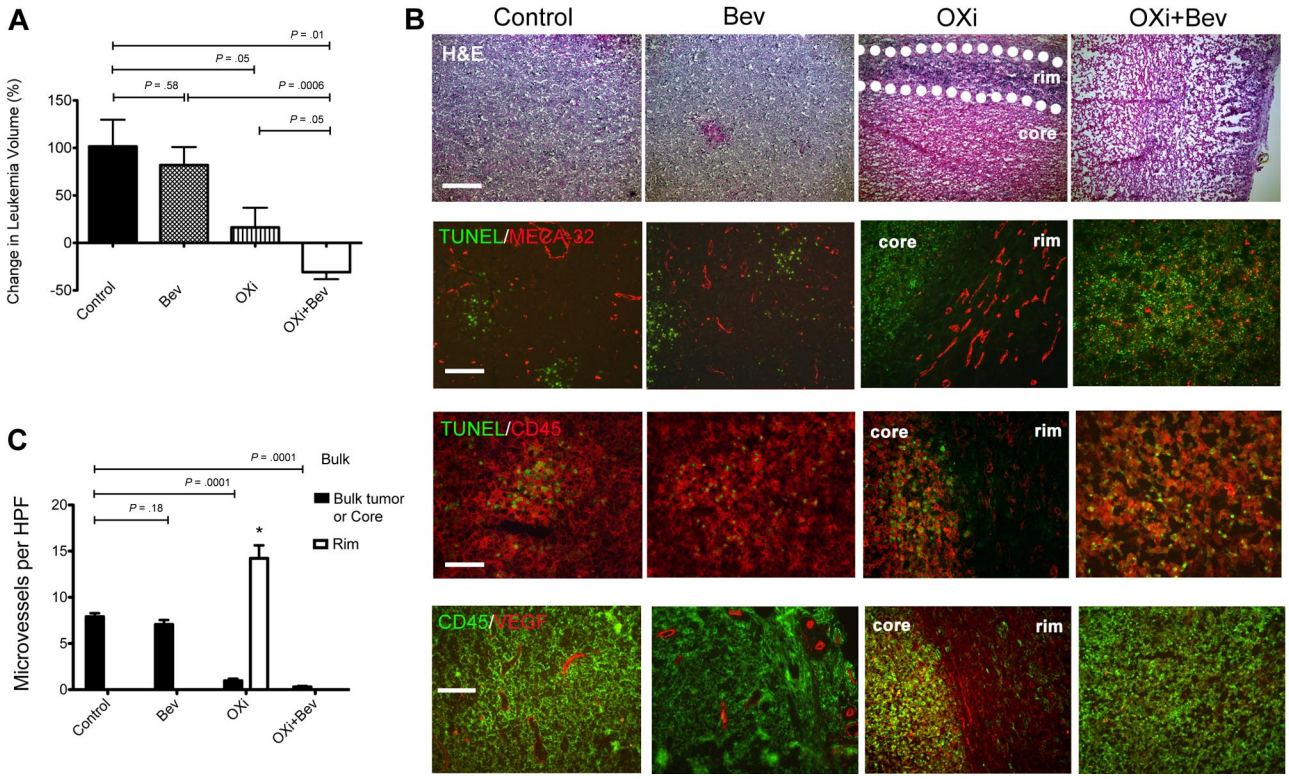

Figure 1. Effects of OXi4503 and bevacizumab on subcutaneous leukemic chloromas. NOD/scid/IL2Rγ$^{-/-}$ (NOG) mice were subcutaneously inoculated with KG-1 human acute myelogenous leukemia (AML) cells. After chloromas were palpable mice were treated with intraperitoneal injections of bevacizumab, OXi4503, combination (OXi+Bev), or controls. Leukemia growth was measured every other day. (A) OXi4503 alone decreased leukemia growth in comparison to controls. Combination Oxi4503+Bev treatment resulted in regression of cancer size. Bevacizumab alone had no effect on tumor growth. (B) Comprehensive staining of chloromas was performed for: H&E (scale bar: 200 μm), TUNEL/MECA-32 (scale bar: 100 μm), (TUNEL/CD45 (scale bar: 50 μm), and CD45/VEGF-A (scale bar: 100 μm). Sections showed that OXi4503 monotherapy led to chloromas with central cores made up mainly of nonvascularized, TUNEL$^+$ apoptotic cells and viable rims (outlined by dotted lines) containing MECA-32$^+$ blood vessels at the periphery of leukemias. VEGF-A expression was also observed in viable rims. Combination therapy eliminated the viable rim resulting in widespread apoptosis and a lack of intact blood vessels throughout the tumor mass. Bevacizumab-treated tumors showed no difference in staining compared with controls. (C) Quantification of microvessels based on MECA-32$^+$ blood vessels revealed decreased density within leukemic cores of mice treated with OXi4503 and combination therapy in comparison to bulk control tumors. Blood vessels within viable leukemia rims are increased after OXi4503 treatment but significantly decreased with additional bevacizumab treatment. Values represent mean ± SEM. *$P < .05$.

Results

OXi4503 regresses leukemia in an in vivo subcutaneous chloroma model

To investigate the effects of OXi4503 on leukemia proliferation in vivo, we first established KG-1 subcutaneous chloromas in NOG mice. After 28 days when tumors were palpable, OXi4503 was injected intraperitoneally at a dose of 10 mg/kg 3 times a week for 2 weeks. Chloromas were measured every other day and volumes calculated. KG-1 tumors in mice treated with OXi4503 grew significantly slower after treatment compared with control animals ($P = .05$; n = 5; Figure 1A). Furthermore, H&E staining showed that OXi4503-treated chloromas developed a central core of necrotic cells with a surrounding rim of viable tissue (Figure 1B). Viable rims were easily identified on gross and microscopic sections. To gain further insight into the mechanism of OXi4503-induced leukemia cell death in vivo, TUNEL staining was performed given that OXi4503 contains an ortho-quinone species capable of generating intracellular ROS. Control chloromas consisted of a homogenous presentation of viable leukemia cells with minimal signs of apoptosis (Figure 1B). In contrast, OXi4503-treated chloromas showed increased TUNEL staining within the core, consistent with widespread cellular apoptosis (Figure 1B). To appreciate the vascular disrupting effects of OXi4503 given its microtubule targeting capability, microvessel staining was performed using antibodies to MECA-32. In KG-1–bearing mice treated with OXi4503, necrotic cores revealed very few, if any, blood vessels while viable rims remained rich in blood vessels (Figure 1B). Compared with bulk control leukemias, OXi4503-treated leukemias showed significantly decreased microvessel densities within leukemic cores ($P < .0001$; n = 10; Figure 1C); however, viable rims showed increased microvessel density potentially due to a reactive angiogenic response to OXi4503 treatment ($P < .01$; n = 10; Figure 1C). Interestingly, TUNEL staining was mainly associated with CD45$^+$ leukemia cells and not with MECA-32$^+$ blood vessels in control or bevacizumab-treated chloromas. These data suggest that targeting leukemia xenografts with OXi4503 leads to leukemia regression via vascular disruption and apoptotic mechanisms. However, the maintenance of a highly vascularized viable rim with higher microvessel density versus controls suggested that a robust reactive angiogenic process[36] was activated in the rims in response to the effects of OXi4503.

Inhibiting angiogenesis with vascular disruption enhances leukemia regression

Given the observed reactive angiogenic process and persistence of a viable leukemic rim after OXi4503 monotherapy in the subcutaneous chloroma model, we focused on inhibiting VEGF activity considering its important role in tumor angiogenesis.[37-39] Initially,

KG-1 tumors were established in NOG mice and bevacizumab was administered alone at a dose of 4 mg/kg intraperitoneally weekly for 2 weeks. Chloromas were measured every other day for volume calculations. KG-1 tumors in bevacizumab-treated mice (n = 5) grew at the same rate compared with control animals ($P = .58$; Figure 1A). In addition, the bevacizumab-treated chloromas showed no histologic differences to controls based on gross examination and H&E staining, with no delineation between a central necrotic core and viable rim (Figure 1B). Instead, bevacizumab-treated leukemias were viable throughout the entire tumor. TUNEL staining showed similar levels of apoptosis of $CD45^+$ cells in bevacizumab-treated leukemias in relation to controls tumors (Figure 1B). In regard to vascular assessments, MECA-32^+ blood vessels were found throughout leukemias of bevacizumab-treated mice, which was again similar to controls (Figure 1B). There were no differences in microvessel densities between bevacizumab-treated and control cohorts ($P = .18$; n = 5; Figure 1C). Together, these data suggest that treatment with bevacizumab alone does not significantly impact chloroma growth, viability, and vascularity.

To begin to define the mechanism driving reactive angiogenesis in the viable rims, we next stained the different chloromas with antibodies for VEGF-A. Interestingly, in control and bevacizumab-treated leukemias VEGF-A staining was found throughout the tumor mass mainly associated with viable blood vessels (Figure 1B). Conversely, in OXi4503-treated chloromas, VEGF-A staining was highly expressed in the viable rim with some staining observed in the apoptotic core (Figure 1B). Again, VEGF-A staining was associated with intact blood vessels. These data suggested that the reactive angiogenic process was mediated via VEGF-A production from blood vessels found within the viable rim.

Having established the formation of viable rims in OXi4503 alone treated chloromas and the high levels of VEGF-A expression in the viable rims, we next tested the combination of OXi4503 and bevacizumab in leukemia. We hypothesized that bevacizumab would mitigate the VEGF-mediated reactive angiogenesis process after OXi4503 treatment and lead to further leukemia regression, especially in relation to the observed viable rim. To evaluate the effect of combination bevacizumab and OXi4503, KG-1–bearing mice were treated with OXi4503 (10 mg/kg intraperitoneally 3 times a week) and bevacizumab (4 mg/kg intraperitoneally weekly) for 2 weeks (n = 10). Chloromas were measured every other day and volumes calculated. Interestingly, KG-1 tumors in combination-treated mice regressed in overall size and were significantly smaller in comparison to control mice ($P = .01$) as well as bevacizumab monotherapy treated mice ($P = .0006$; Figure 1A). There was also a significant trend toward decreased growth in combination-treated mice compared with OXi4503 monotherapy–treated mice ($P = .05$; Figure 1A). In addition, the chloromas in combination-treated mice were softer to palpation and were mainly necrotic without a persistent viable rim as observed with the OXi4503 alone treatments (Figure 1B). TUNEL staining revealed widespread apoptosis throughout the entire leukemic mass (Figure 1B). MECA-32 staining showed almost complete elimination of blood vessels within chloromas treated with combination OXi4503 plus bevacizumab (Figure 1B). Microvessel density in leukemias after combination treatment was markedly decreased compared with control cohorts ($P < .0001$) as well as bevacizumab-treated ($P < .0001$) and core of OXi4503-treated ($P = .005$) chloromas (Figure 1C). Finally, VEGF-A staining showed nondetectable levels of VEGF-A throughout the tumor mass. Together, these data suggest that targeting leukemia xenografts with a combination of OXi4503 and bevacizumab leads to an enhanced leukemia regression via apoptotic mechanisms and abrogation of reactive angiogenesis in the viable rims.

OXi4503 induces bone marrow remissions in high-risk AML model

To test the effects of OXi4503 and bevacizumab in a setting that more closely resembles the clinical presentation of leukemic infiltration in bone marrow, we used a systemic leukemia model. Here, we used AML samples from various AML subtypes (M1/2, M2, M4, and M5; Table 1) including primary human AML specimens that harbored the high-risk FLT3 ITD mutation. Irradiated NOG mice were transplanted intravenously (IV) with 10 to 50×10^6 AML cells and examined at 6 to 8 weeks to measure leukemia engraftment. Mice were randomly assigned to 1 of 4 treatment groups: 2 weeks of bevacizumab alone (n = 6; 4 mg/kg intraperitoneally weekly), OXi4503 alone (n = 8; 10 mg/kg intraperitoneally 3 times a week), combination of OXi4503 and bevacizumab at the same dosing regimens (n = 11) or control (n = 7). AML engraftment in the bone marrow of bevacizumab-treated mice was comparable with control mice ($P = .7914$) with all 6 mice showing engraftment by flow cytometry (Figure 2A-B). Mice treated with OXi4503 monotherapy resulted in a significant decrease of AML in bone marrow compared with controls ($P = .0033$) with only 1 of 8 OXi4503-treated mice showing engraftment by flow cytometry (Figure 2A-B). In animals treated with combination OXi4503 and bevacizumab, 1 of 11 animals showed AML engraftment by flow cytometry with the overall levels of engraftment being significantly lower than controls ($P = .0038$; Figure 2A-B). To more rigorously test for molecular remission we used PCR to examine the effects of treatment on the FLT3 ITD^+ AML M1/2 subtype. Molecular remissions were evident in both OXi4503 monotherapy and combination-treated mice but not in any of the control and bevacizumab-treated animals (Figure 2C). These data indicate that OXi4503 and the combination of OXi4503 plus bevacizumab result in phenotypic and molecular remissions of high-risk primary AML.

To test whether bevacizumab treatment had any effect, staining was performed on the bone marrow of bevacizumab-treated mice. $CD45^+$ cells were evident in mouse bone marrow supporting the flow cytometric data, whereas TUNEL staining showed a general lack of apoptosis throughout the bone sections (Figure 2D). Positive staining with HIF-1α indicated that bevacizumab treatment did mediate a hypoxic response, which was not observed in control mice (Figure 2E). HIF-1α staining was mainly associated with $CD45^+$ leukemic cells and not MECA-32^+ blood vessels (Figure 2E). No CD45, TUNEL, or VEGF-A staining was observed, with minimal HIF-1α staining, in OX4503 or OXi4503 plus bevacizumab-treated mice (data not shown). These data suggest that bevacizumab may have generated hypoxic conditions in the bone marrow to elicit a HIF-1α response, which was not observed in control mice. However, this effect was not substantial enough to eliminate leukemic engraftment or to overcome the known protective effects of HIF-1α when tissues are under hypoxic conditions.[40]

To gain further insight into mechanisms involved in leukemia remissions after OXi4503 treatment, bone marrow sections were further analyzed. Blood vessels were detected by MECA-32 staining and revealed intact blood vessels in the bone marrow of all treatment groups (Figure 3A). TUNEL staining showed little or undetectable levels of apoptosis in all groups indicating that the AML eliminating effects of OXi4503 was complete at the time of analysis (Figure 3A). Microvessel density was then determined for

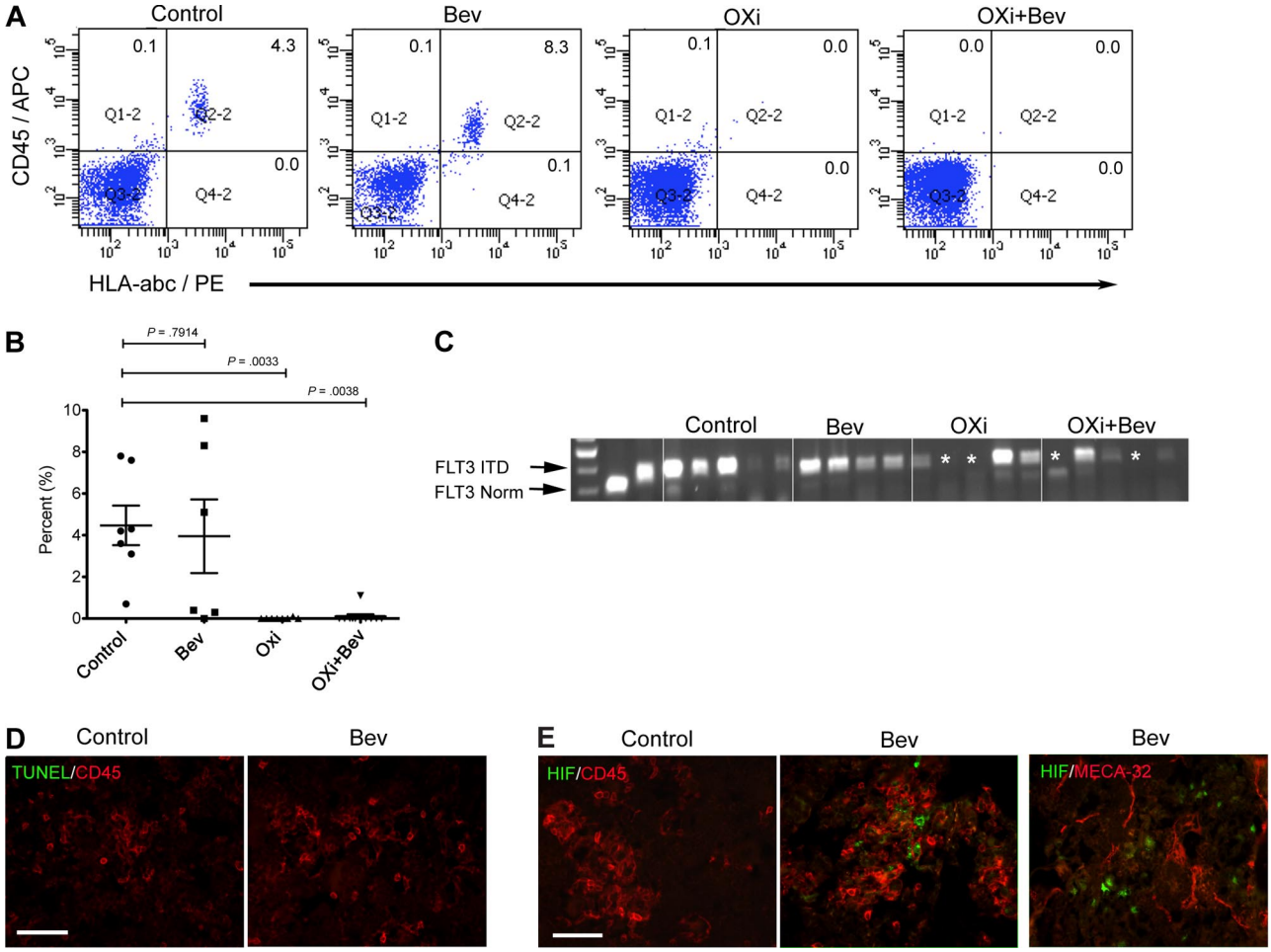

Figure 2. OXi4503 induced regression of systemic AML in bone marrow. Irradiated NOG mice were transplanted with human AML of differing subtypes (M1/2, M4, and M5) including a primary human AML specimen that harbored a high-risk FLT3 ITD mutation and after verification of leukemia engraftment were randomly assigned to 1 of 4 treatment cohorts. (A) Six weeks after AML transplant, NOG mice were treated with bevacizumab, OXi4503, combination (OXi4503+Bev), or controls. After 2 weeks of treatment, bone marrow showed persistence of AML in control and bevacizumab-treated mice. However, incidences of AML engraftment were significantly decreased with OXi4503 (1/8 positive) and combination treatment (1/11 positive) in comparison to controls. Shown are representative flow cytometric plots showing leukemic engraftment in control and bevacizumab-treated mice and no leukemic engraftment in Oxi4503 and combination-treated mice. (B) Quantification of AML engraftment by flow cytometry showed significantly decreased engraftment in OXi4503 and combination-treated animals versus controls. (C) PCR analysis for FLT3 ITD AML revealed molecular remissions (*) of high-risk FLT3 ITD$^+$ AML in 40% of OXi4503 and combination-treated animals. (D-E) TUNEL staining showed no detectable apoptotic response to bevacizumab (D); however, a hypoxia-mediated reaction was observed upon HIF-1α staining (E). CD45$^+$ cells were observed throughout bone marrow sections (scale bar: 100 μm). Values represent mean $\pm$ SEM. Gating was established using appropriate isotype controls.

each treatment group plus an additional control group that did not receive leukemia transplant. Enumeration of vessel densities showed that the control (+)leukemia group had significantly higher vessel densities versus control (−)leukemia cohorts, demonstrating that leukemia causes an increase in blood vessels within the bone marrow, which has been previously observed in patient samples (Figure 3B; $*P < .05$).[5-9] Compared with the control (−)leukemia group, bevacizumab and OXi4503 alone treated groups showed significantly higher bone marrow vessel densities while the OXi4503 plus bevacizumab marrows showed lower microvessel densities (Figure 3B; $*P < .05$). In comparison to the control (+)leukemia cohort, all 3 treatment groups showed significantly lower microvessel densities (Figure 3B; $**P < .05$). The combination of OXi4503 plus bevacizumab treatment resulted in a further decrease in microvessel density in comparison to bevacizumab alone ($***P < .05$) or OXi4503 alone ($****P < .05$) groups (Figure 3B).

The finding that microvessel density was similar between bevacizumab alone and OXi4503 alone groups, even though OXi4503 alone treatment mediated leukemia regression, suggested that OXi4503 may have additionally acted through a targeted effect on leukemia cells. To test this theory, the direct toxic effects of OXi4503 on leukemia were determined using KG-1 cells at input cell numbers ranging from 1×10^5 to 2×10^6. In these in vitro studies, OXi4500, the active, de-phosphorylated form of OXi4503 was used.[30-34] OXi4500 was directly cytotoxic to the leukemia cells in a concentration dependent manner with 50nM or higher OXi4500 needed to observe a significant decrease in viable cell number versus controls (Figure 3C). Staining with annexin V and PI identified apoptosis as the main cause of cell death after exposure to OXi4500 (Figure 3D). As expected, concentrations of 50nM or higher elicited more robust apoptotic responses to OXi4500 at 24 hours, as did an additional 24-hour incubation (48 hours total) at corresponding concentrations (Figure 3D). A small population of annexin V$^-$ PI$^+$ cells was observed in all groups indicating that OXi4500 mediated cell death was mainly due to apoptosis. Finally, given the ability of OXi4500 to be oxidized into a reactive ortho-quinone,[30-34] we next determined whether the production of ROS coincided with KG-1 cell death. Here we observed high levels

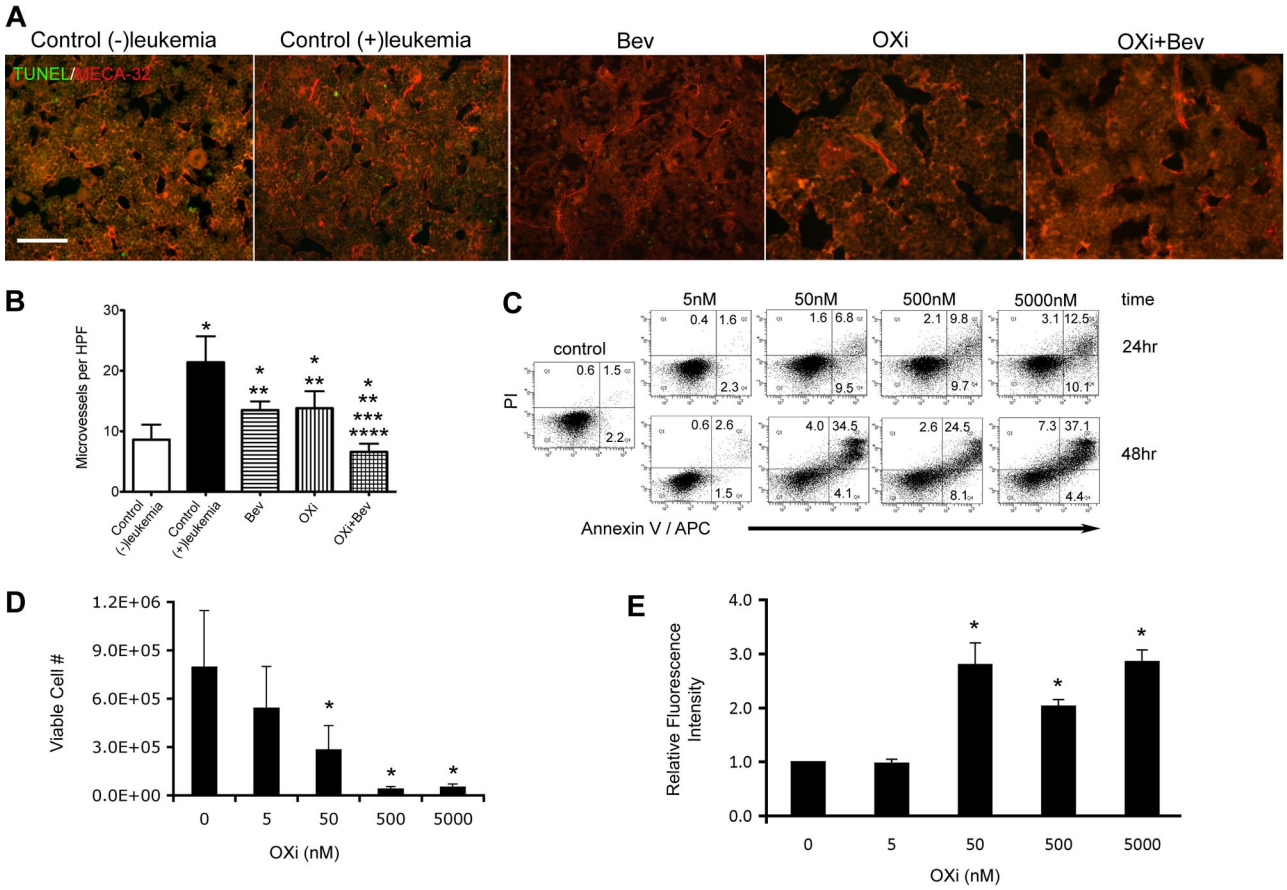

Figure 3. Effects of OXi4503 treatment on bone marrow blood vessels and leukemia cells. (A) MECA-32 staining demonstrated abundant blood vessels throughout bone marrow sections regardless of treatment type (scale bar: 50 μm). (B) Quantification of microvessel density was performed for all treatment and control groups. An additional control group without leukemia transplantation was added to assess the effects of leukemia on microvessel density. * represents significance in comparison to control (−)leukemia group; **, significance in comparison to control (+)leukemia group; ***, significance in comparison to bevacizumab alone group; and ****, significance in comparison to OXi4503 alone group. (C) Leukemic KG-1 cells were incubated with OXi4500 at differing concentrations for 24 hours and the numbers of viable cells quantified using trypan blue dye exclusion. Under these conditions, concentrations of 50nM or higher showed significant decreases in cell viability versus controls. (D) OXi4500 treatment induces apoptosis of leukemic KG-1 cells. After a 24-hour treatment with OXi4500, cells were stained with annexin V and PI and the percentage of apoptotic cells determined using flow cytometry. (E) The generation of ROS was assessed in KG-1 cells at different OXi4500 concentrations by H2DCFDA staining. After 48 hours, ROS were detected at concentrations of 50nM or higher. Relative fluorescent intensity values were normalized to controls (0nM OXi4500). Values represent mean ± SEM; *$P < .05$; **$P < .05$; ***$P < .05$; and ****$P < .05$. Gating was established using appropriate isotype controls.

of ROS production when cells were exposed to 50nM or higher concentrations of OXi4500 for 48 hours, which coincided with the concentration and time of exposure that resulted in cell death due to apoptosis (Figure 3E). Together, these data suggest that OXi4503 additionally induced in vivo leukemia elimination by direct cytotoxicity in a concentration-dependent and time-dependent manner via generation of ROS resulting in apoptosis.

Discussion

Leukemia survival and proliferation depend on interactions with endothelial cells. Soluble mediators secreted by endothelial cells and cell-cell interactions with endothelial cells protect leukemia cells from apoptosis and promote propagation.[10-12] Clinically, increased angiogenesis, noted by an increase in microvessel density, is evident in the bone marrow of patients with AML.[15,41] Endothelial cells may also protect leukemia cells from cytotoxic chemotherapies.[42,43] In reciprocal fashion, endothelial cells are supported and promoted by leukemia cells.[17] Given this codependent relationship, we tested a novel antivascular agent (OXi4503) to treat AML. We found that OXi4503 was capable of eliminating already established leukemia in vivo, whereas the addition of bevacizumab was required to abrogate reactive angiogenesis after OXi4503 treatment of leukemic chloromas.

Various single-agent antivascular strategies have been tested previously in AML; however, their major limitation has been a lack of potency in targeting leukemic blood vessels. Anti-VEGF monotherapy with bevacizumab has been tested in patients with relapsed and refractory AML, and resulted in a decrease in cellular VEGF expression without antileukemic activity.[20] Administering bevacizumab as Timed Sequential Therapy (TST) immediately after cytoreductive therapy resulted in decreased marrow microvessel density, decreased serum VEGF levels and durable complete remissions in 33% of patients, which is comparable with other TSTs.[19] However, no randomized trials examining the additive effects of bevacizumab have as yet been performed. In our study, results from cohorts receiving bevacizumab alone confirm prior reports of no disease eradication and minimal changes in pathobiology.

There has been increasing enthusiasm over targeting interactions among angiopoietin 1 (Ang-1), Ang-2 and Tie-2, given evidence that leukemia cells and endothelial cells use these crosstalk factors for mutual survival and proliferation.[44-46] Bone

marrow expression of Ang-2, a Tie-2 antagonist, has favorable prognostic impact on the overall survival of AML patients, suggesting that the Ang-1/Tie-2 interaction may be important in AML progression.[6,47] Based on these findings, Tie-2 inhibitors, such as AMG 386 (Amgen), a selective angiopoietin-1/-2-neutralizing peptibody, are being developed clinically.

In search of a novel treatment strategy of interfering with multiple critical interactions between endothelial cells and leukemia cells, we reasoned that an optimal strategy would be to target both cell populations, thereby eliminating multiple pathways in their codependent relationship. Therefore, we focused on evaluating a novel VDA in the treatment of leukemia. A first-generation combretastatin, CA4P, was previously reported to exhibit antileukemic effects in cell lines via vascular disruption and mitochondrial toxicity.[29] This agent is currently undergoing phase 2/3 clinical evaluation in solid tumors.[48] Recently, a new combretastatin, OXi4503, was identified as having enhanced antitumor activity in solid tumor models.[30-35] Results from our study also show that OXi4503 is a potent antileukemic agent.

In our chloroma model, OXi4503 resulted in significant reduction of leukemia growth with decreased microvessel density. However, after OXi4503 monotherapy we also detected viable rims of leukemia cells and reactive angiogenesis in the chloromas. Analysis of viable rim tissues revealed active VEGF-A activity so it was a logical extension to administer adjuvant bevacizumab. When we treated chloromas with a combination of bevacizumab and OXi4503 we found complete elimination of the viable rim of leukemia cells, decreased microvessels and widespread apoptosis. This finding is consistent with our prior reports of VDA application in solid tumors and suggests that treatment with OXi4503 may increase the susceptibility of tumor vessels to bevacizumab.[32,35] With these observations, we concluded that leukemic chloromas respond to VDAs in a similar manner to solid tumors including renal cell carcinomas and Kaposi sarcoma.[36,49]

However, we were also interested in evaluating VDA strategies in situations more closely representative of typical AML clinical presentations. Using our systemic model of primary AML, we found that OXi4503 alone possessed the potential to regress established AML of differing subtypes from bone marrow, while bevacizumab alone had no effect. OXi4503 monotherapy resulted in decreased levels of leukemia engraftment both at phenotypic and molecular levels (using a FLT3 ITD mutant AML) and decreased microvessel density in comparison to control (+)leukemia cohorts. Interestingly, bone marrow microvessel densities were similar between bevacizumab and OXi4503 alone treated groups even though OXi4503 alone was able to eliminate leukemia in mice. Furthermore, the rate of phenotypic and molecular remissions between OXi4503 alone and OXi4503 plus bevacizumab groups did not differ significantly, even though the addition of bevacizumab resulted in a more significant decrease in microvessel density. Overall, these observations suggest that the singular effect of decreasing microvessel density does not account for the observed leukemia regression in our systemic model and that other interactions between leukemia and blood vessels play a role in the progression of the disease. Here we show that these interactions are not solely mediated by VEGF-A, given the lack of response to bevacizumab, but are susceptible to OXi4503 disruption. Previous reports suggest that this interaction may occur through cell adhesion molecules such as VCAM.[29] Of note, the molecular remissions of the FLT3 ITD AML observed in this study were enticing because this is a notoriously chemotherapy insensitive leukemia.

In these studies we also observed that OXi4500, the active, de-phosphorylated form of OXi4503, was directly cytotoxic to leukemia cells. Furthermore, this cytotoxicity was dependent on both concentration and time of exposure. At optimal concentrations of 50nM or higher, OXi4500 generated intracellular ROS resulting in apoptosis in 24 to 48 hours in vitro.

Based on these findings, we postulated that the mechanisms by which OXi4503 alone treatment leads to AML remission in vivo is due to 2 major effects: (1) vascular disruption that interferes with endothelial cell interactions with leukemia, and (2) direct cytotoxic effects on leukemia cells via generation of intracellular ROS.

Clinically, OXi4503 is currently under investigation in early phase clinical trials of advanced solid tumors. This agent has not caused significant hematologic toxicity as seen with other microtubule targeting agents such as vinca alkaloids, taxanes, and colchicine. The data presented in this study indicate that OXi4503 may represent a promising therapeutic agent for patients with AML, even those classified with high-risk disease. Whereas we provide initial evidence of OXi4503's potential therapeutic efficacy in AML, additional primary specimens will be required to determine responsiveness with respect to AML disease classifications.

Acknowledgments

The authors thank Sharon Lepler, Rodney Pettway, Clay Bennett, and Sean Haghgou for technical assistance. We are also appreciative for the assistance and insight from Dai Chaplin, Bronwyn Slim, and Kevin Pinney. The authors also thank the patients who donated leukemia specimens; physician assistants, nurse practitioners, and fellows who acquired specimens; and the Shands Stem Cell Laboratory for processing specimens.

This work was supported by the Leukemia & Lymphoma Society 6264-08 (C.R.C.) and the National Institutes of Health (NIH) K08 DK067359 (C.R.C.), NIH R01 HL070738 (E.W.S.), NIH CA089655 (D.W.S.), and NIH CA084408 (D.W.S.).

Authorship

Contribution: G.J.M and C.R.C. contributed to conception of hypotheses, experimental design, execution of experiments, data analysis, and manuscript preparation; D.W.S. and E.W.S. contributed to conception of hypotheses, experimental design, data analysis, and manuscript preparation; and A.M.M., K.H., S.M., and M.J. contributed to execution of experiments.

Conflict-of-interest disclosure: D.W.S. is on the scientific advisory board for Oxigene. The remaining authors declare no competing financial interests.

Correspondence: Christopher R. Cogle, MD, 1600 SW Archer Rd, Box 100278, Gainesville, FL 32610-0278; e-mail: c@ufl.edu.

References

1. Kottaridis PD, Gale RE, Frew ME, et al. The presence of a FLT3 internal tandem duplication in patients with acute myeloid leukemia (AML) adds important prognostic information to cytogenetic risk group and response to the first cycle of chemotherapy: analysis of 854 patients from the United Kingdom Medical Research Council AML 10 and 12 trials. *Blood.* 2001;98(6):1752-1759.

2. Schnittger S, Schoch C, Dugas M, et al. Analysis of FLT3 length mutations in 1003 patients with acute myeloid leukemia: correlation to cytogenetics, FAB subtype, and prognosis in the AMLCG

study and usefulness as a marker for the detection of minimal residual disease. *Blood.* 2002; 100(1):59-66.

3. Tallman MS, Gilliland DG, Rowe JM. Drug therapy for acute myeloid leukemia. *Blood.* 2005; 106(4):1154-1163.
4. Stone RM, DeAngelo DJ, Klimek V, et al. Patients with acute myeloid leukemia and an activating mutation in FLT3 respond to a small-molecule FLT3 tyrosine kinase inhibitor, PKC412. *Blood.* 2005;105(1):54-60.
5. Aguayo A, Estey E, Kantarjian H, et al. Cellular vascular endothelial growth factor is a predictor of outcome in patients with acute myeloid leukemia. *Blood.* 1999;94(11):3717-3721.
6. Loges S, Heil G, Bruweleit M, et al. Analysis of concerted expression of angiogenic growth factors in acute myeloid leukemia: expression of angiopoietin-2 represents an independent prognostic factor for overall survival. *J Clin Oncol.* 2005;23(6):1109-1117.
7. Korkolopoulou P, Apostolidou E, Pavlopoulos PM, et al. Prognostic evaluation of the microvascular network in myelodysplastic syndromes. *Leukemia.* 2001;15(9):1369-1376.
8. Rabitsch W, Sperr WR, Lechner K, et al. Bone marrow microvessel density and its prognostic significance in AML. *Leuk Lymphoma.* 2004; 45(7):1369-1373.
9. Kuzu I, Beksac M, Arat M, et al. Bone marrow microvessel density (MVD) in adult acute myeloid leukemia (AML): therapy induced changes and effects on survival. *Leuk Lymphoma.* 2004;45(6):1185-1190.
10. Hatfield K, Ryningen A, Corbascio M, Bruserud O. Microvascular endothelial cells increase proliferation and inhibit apoptosis of native human acute myelogenous leukemia blasts. *Int J Cancer.* 2006;119(10):2313-2321.
11. Stucki A, Rivier AS, Gikic M, et al. Endothelial cell activation by myeloblasts: molecular mechanisms of leukostasis and leukemic cell dissemination. *Blood.* 2001;97(7):2121-2129.
12. Bistrian R, Dorn A, Mobest DC, et al. Shear stress-mediated adhesion of acute myeloid leukemia and KG-1 cells to endothelial cells involves functional P-selectin. *Stem Cells Dev.* 2009;18(8): 1235-1242.
13. Perez-Atayde AR, Sallan SE, Tedrow U, et al. Spectrum of tumor angiogenesis in the bone marrow of children with acute lymphoblastic leukemia. *Am J Pathol.* 1997;150(3):815-821.
14. Fiedler W, Graeven U, Ergun S, et al. Vascular endothelial growth factor, a possible paracrine growth factor in human acute myeloid leukemia. *Blood.* 1997;89(6):1870-1875.
15. Hussong JW, Rodgers GM, Shami PJ. Evidence of increased angiogenesis in patients with acute myeloid leukemia. *Blood.* 2000;95(1):309-313.
16. Padró T, Ruiz S, Bieker R, et al. Increased angiogenesis in the bone marrow of patients with acute myeloid leukemia. *Blood.* 2000;95(8):2637-2644.
17. Hatfield K, Oyan AM, Ersvaer E, et al. Primary human acute myeloid leukaemia cells increase the proliferation of microvascular endothelial cells through the release of soluble mediators. *Br J Haematol.* 2009;144(1):53-68.
18. Fiedler W, Mesters R, Tinnefeld H, et al. A phase 2 clinical study of SU5416 in patients with refractory acute myeloid leukemia. *Blood.* 2003;102(8): 2763-2767.
19. Karp JE, Gojo I, Pili R, et al. Targeting vascular endothelial growth factor for relapsed and refractory adult acute myelogenous leukemias: therapy with sequential 1-beta-d-arabinofuranosylcytosine, mitoxantrone, and bevacizumab. *Clin Cancer Res.* 2004;10(11):3577-3585.
20. Zahiragic L, Schliemann C, Bieker R, et al. Bevacizumab reduces VEGF expression in patients with relapsed and refractory acute myeloid leukemia without clinical antileukemic activity. *Leukemia.* 2007;21(6):1310-1312.
21. Dias S, Hattori K, Zhu Z, et al. Autocrine stimulation of VEGFR-2 activates human leukemic cell growth and migration. *J Clin Invest.* 2000;106(4): 511-521.
22. Dias S, Hattori K, Heissig B, et al. Inhibition of both paracrine and autocrine VEGF/ VEGFR-2 signaling pathways is essential to induce long-term remission of xenotransplanted human leukemias. *Proc Natl Acad Sci U S A.* 2001;98(19): 10857-10862.
23. Dark GG, Hill SA, Prise VE, et al. Combretastatin A-4, an agent that displays potent and selective toxicity toward tumor vasculature. *Cancer Res.* 1997;57(10):1829-1834.
24. Siemann DW, Chaplin DJ, Horsman MR. Vascular-targeting therapies for treatment of malignant disease. *Cancer.* 2004;100(12):2491-2499.
25. Chaplin DJ, Pettit GR, Hill SA. Anti-vascular approaches to solid tumour therapy: evaluation of combretastatin A4 phosphate. *Anticancer Res.* 1999;19(1A):189-195.
26. Grosios K, Holwell SE, McGown AT, Pettit GR, Bibby MC. In vivo and in vitro evaluation of combretastatin A-4 and its sodium phosphate prodrug. *Br J Cancer.* 1999;81(8):1318-1327.
27. Galbraith SM, Chaplin DJ, Lee F, et al. Effects of combretastatin A4 phosphate on endothelial cell morphology in vitro and relationship to tumour vascular targeting activity in vivo. *Anticancer Res.* 2001;21(1A):93-102.
28. Kanthou C, Tozer GM. The tumor vascular targeting agent combretastatin A-4-phosphate induces reorganization of the actin cytoskeleton and early membrane blebbing in human endothelial cells. *Blood.* 2002;99(6):2060-2069.
29. Petit I, Karajannis MA, Vincent L, et al. The microtubule-targeting agent CA4P regresses leukemic xenografts by disrupting interaction with vascular cells and mitochondrial-dependent cell death. *Blood.* 2008;111(4):1951-1961.
30. Hill SA, Toze GM, Pettit GR, Chaplin DJ. Preclinical evaluation of the antitumour activity of the novel vascular targeting agent Oxi 4503. *Anticancer Res.* 2002;22(3):1453-1458.
31. Hua J, Sheng Y, Pinney KG, et al. Oxi4503, a novel vascular targeting agent: effects on blood flow and antitumor activity in comparison to combretastatin A-4 phosphate. *Anticancer Res.* 2003; 23(2B):1433-1440.
32. Salmon HW, Siemann DW. Effect of the second-generation vascular disrupting agent OXi4503 on tumor vascularity. *Clin Cancer Res.* 2006;12(13): 4090-4094.
33. Lippert JW III. Vascular disrupting agents. *Bioorg Med Chem.* 2007;15(2):605-615.
34. Folkes LK, Christlieb M, Madej E, Stratford MR, Wardman P. Oxidative metabolism of combretastatin A-1 produces quinone intermediates with the potential to bind to nucleophiles and to enhance oxidative stress via free radicals. *Chem Res Toxicol.* 2007;20(12):1885-1894.
35. Siemann DW, Horsman MR. Vascular targeted therapies in oncology. *Cell Tissue Res.* 2009;335(1): 241-248.
36. Siemann DW, Shi W. Dual targeting of tumor vasculature: combining Avastin and vascular disrupting agents (CA4P or OXi4503). *Anticancer Res.* 2008;28(4B):2027-2031.
37. Connolly DT, Heuvelman DM, Nelson R, et al. Tumor vascular permeability factor stimulates endothelial cell growth and angiogenesis. *J Clin Invest.* 1989;84(5):1470-1478.
38. Shweiki D, Itin A, Soffer D, Keshet E. Vascular endothelial growth factor induced by hypoxia may mediate hypoxia-initiated angiogenesis. *Nature.* 1992;359(6398):843-845.
39. Kim KJ, Li B, Winer J, et al. Inhibition of vascular endothelial growth factor-induced angiogenesis suppresses tumour growth in vivo. *Nature.* 1993; 362(6423):841-844.
40. Pugh CW, Ratcliffe PJ. Regulation of angiogenesis by hypoxia: role of the HIF system. *Nat Med.* 2003;9(6):677-684.
41. Padró T, Bieker R, Ruiz S, et al. Overexpression of vascular endothelial growth factor (VEGF) and its cellular receptor KDR (VEGFR-2) in the bone marrow of patients with acute myeloid leukemia. *Leukemia.* 2002;16(7):1302-1310.
42. Dias S, Choy M, Alitalo K, Rafii S. Vascular endothelial growth factor (VEGF)-C signaling through FLT-4 (VEGFR-3) mediates leukemic cell proliferation, survival, and resistance to chemotherapy. *Blood.* 2002;99(6):2179-2184.
43. Liesveld JL, Rosell KE, Lu C, et al. Acute myelogenous leukemia–microenvironment interactions: role of endothelial cells and proteasome inhibition. *Hematology.* 2005;10(6):483-494.
44. Hatfield KJ, Hovland R, Oyan AM, et al. Release of angiopoietin-1 by primary human acute myelogenous leukemia cells is associated with mutations of nucleophosmin, increased by bone marrow stromal cells and possibly antagonized by high systemic angiopoietin-2 levels. *Leukemia.* 2008;22(2):287-293.
45. Riccioni R, Diverio D, Mariani G, et al. Expression of Tie-2 and other receptors for endothelial growth factors in acute myeloid leukemias is associated with monocytic features of leukemic blasts. *Stem Cells.* 2007;25(8):1862-1871.
46. Reikvam H, Hatfield KJ, Lassalle P, et al. Targeting the angiopoietin (Ang)/Tie-2 pathway in the crosstalk between acute myeloid leukaemia and endothelial cells: studies of Tie-2 blocking antibodies, exogenous Ang-2 and inhibition of constitutive agonistic Ang-1 release. *Expert Opin Investig Drugs.* 19(2):169-183.
47. Schliemann C, Bieker R, Padro T, et al. Expression of angiopoietins and their receptor Tie2 in the bone marrow of patients with acute myeloid leukemia. *Haematologica.* 2006;91(9):1203-1211.
48. Siemann DW, Chaplin DJ, Walicke PA. A review and update of the current status of the vasculature-disabling agent combretastatin-A4 phosphate (CA4P). *Expert Opin Investig Drugs.* 2009;18(2):189-197.
49. Rojiani AM, Li L, Rise L, Siemann DW. Activity of the vascular targeting agent combretastatin A-4 disodium phosphate in a xenograft model of AIDS-associated Kaposi's sarcoma. *Acta Oncol.* 2002;41(1):98-105.